

Groundwater recharge in Brandenburg is declining - but why?

Till Francke^{1,*} and Maik Heistermann^{1,*}

^{1,*}Institute for Environmental Sciences and Geography, University of Potsdam, Potsdam, Germany

*These authors contributed equally to this work.

Correspondence: Maik Heistermann (maik.heistermann@uni-potsdam.de)

Abstract.

Brandenburg is among the driest federal states in Germany, featuring low rates of ~~ground-water~~ groundwater recharge (GWR) across large parts of the state. This GWR is fundamental to both water supply and the support of natural ecosystems. There is strong observational evidence, however, that GWR has been declining since 1980: first, river discharge (which is almost exclusively fed via GWR) has been significantly decreasing in many catchments (by around 40 % since 1980). Second, ~~ground-water~~ groundwater levels in the groundwater recharge areas show a significant long-term decline. In this study, we search for potential reasons behind this decline, by investigating five catchments across Brandenburg that we consider as largely unaffected by direct anthropogenic interference with the water balance. Using the Soil-Water-Atmosphere-Plant model (SWAP) to simulate long-term trends in GWR, we found that significant increases of air temperature, solar irradiation and leaf area index (LAI) since 1980 acted towards a decrease in GWR in the order of -21 to -4 mm a⁻¹ per decade from 1980 to 2023. The Brandenburg-wide LAI trend of +0.1 m² m⁻² per decade was inferred from a recently published, spatio-temporally consistent LAI reconstruction. The contribution of this LAI trend to the decrease of GWR amounted to -5 to -3 mm a⁻¹ per decade. Based on our results, we consider it as very likely that the decrease in discharge since 1980 can be explained by a decrease in GWR which, in turn, was caused by climate change in combination with an increasing LAI. However, we also found that precipitation trends can be highly incoherent at the catchment scale. Even though these precipitation trends are not significant, they can have a fundamental impact on the significance, the magnitude and even on the sign of simulated GWR trends. Given the uncertainty of the precipitation trend, four out of five catchments still appear to exhibit a gap between negative simulated GWR trends and more negative observed discharge trends. We provide a comprehensive discussion of possible reasons and uncertainties to explain this gap, including the effects of the limited length and the inhomogeneity of climate and discharge records, the role of land cover and vegetation change, irrigation water consumption, latent anthropogenic interventions in the catchments water balance, uncertainties in ~~ground-water~~ groundwater table depth, as well as model-related uncertainties. Addressing these uncertainties should be a prime subject for prospective research with regard to the effects of environmental change on GWR in Brandenburg. Water resources management and planning in Brandenburg should, however, already take into account the possibility of GWR to decrease further. Given the fundamental importance of precipitation trends and their large uncertainty in future projections, we strongly advise against putting our hopes in a future increase of GWR as projected mainly on the basis of expected future increases in winter precipitation.

1 Introduction

With average annual precipitation depths between 500 and 700 mm, Brandenburg is among the driest federal states in Germany. At the same time, it heavily relies on water supply from groundwater resources (Landesamt für Umwelt Brandenburg, 2022).

30 While the recharge of these groundwater resources typically takes place in elevated areas of glacial deposits with a ~~distant~~ deep groundwater table, extended lowlands (with ~~elose~~ shallow groundwater tables) exist where high evapotranspiration rates fundamentally reduce or even reverse the net vertical flux of water towards the aquifer.

Any long-term shift of Brandenburg's already unfavourable vertical water balance towards lower rates of net groundwater recharge (GWR) would put water resource management in Brandenburg at risk – including the German capital Berlin in its
35 centre (Somogyvári et al., 2024; Pohle et al., 2025; Somogyvári et al., 2025). And, in fact, there is strong evidence for such a decline: ~~;~~

First, ~~ground-water~~ groundwater levels decreased significantly between 1976 and 2020 in the recharge areas (i.e. in the elevated areas with large distances to the ~~ground-water~~ groundwater table, see Fig. 1). The most plausible hypothesis to explain such a state-wide prevalence of ~~these negative trends can only be explained by negative trends is~~ a declining GWR, since
40 while there is no ~~basis to assume such a widespread abstraction of groundwater from local wells as an alternative explanation.~~ Please note evidence for any wide-spread increase of groundwater abstractions in the past decades. Quite the contrary, water abstractions have considerably decreased, at least since 1991 (Landesamt für Umwelt Brandenburg, 2022). Concerning the groundwater levels, it has to be noted that the lowlands do not show strong trends in either direction because the groundwater level is ~~confined~~ stabilised by the water level of the heavily-regulated streams and rivers to which the aquifers are connected.

45 Second, the discharge of many rivers in Brandenburg has been significantly decreasing since 1980. Fig. 1 shows discharge observations for five river basins (or combinations of such, see section 2.2 for details) that can be considered as largely unaffected by anthropogenic influences such as inter-basin water transfers or open pit mining (which widely occurs in the catchments of the rivers Spree and the Schwarze Elster and involves, in the active phase, pumping of groundwater into rivers, and, in the restoration phase, the flooding of abandoned mining pits from groundwater or surface water, which may dominate groundwater
50 and discharge dynamics, see Kröcher et al., 2025). The discharge series shown in Fig. 1 represent river basins with continuous discharge records since at least 1980, and with upstream catchment areas of at least 500 km², which allows us to assume some level of representativeness for the regional water balance and reduces the sensitivity to uncertainties in belowground catchment areas. According to these records, the decrease in discharge since 1980 is highly significant, corresponding to a rate between
-21 and -10 mm/~~aper decade~~ a⁻¹ per decade ("mm a⁻¹ dec⁻¹" from hereon) and a total loss of around 40 % since 1980. Given
55 the highly permeable soils in Brandenburg and the resulting insignificance of surface runoff (LUA Brandenburg, 2001), the discharge of these catchments can be considered to be almost exclusively fed from groundwater recharge; any long-term decrease of discharge must hence be caused by a declining GWR, given the absence of other dominant processes of anthropogenic interference, as mentioned above.

Certainly, GWR is an elusive variable that is difficult to quantify and impossible to measure directly at the landscape scale.
60 Interestingly, the aforementioned evidence for a decreasing GWR in Brandenburg is in contrast to a recently published mod-

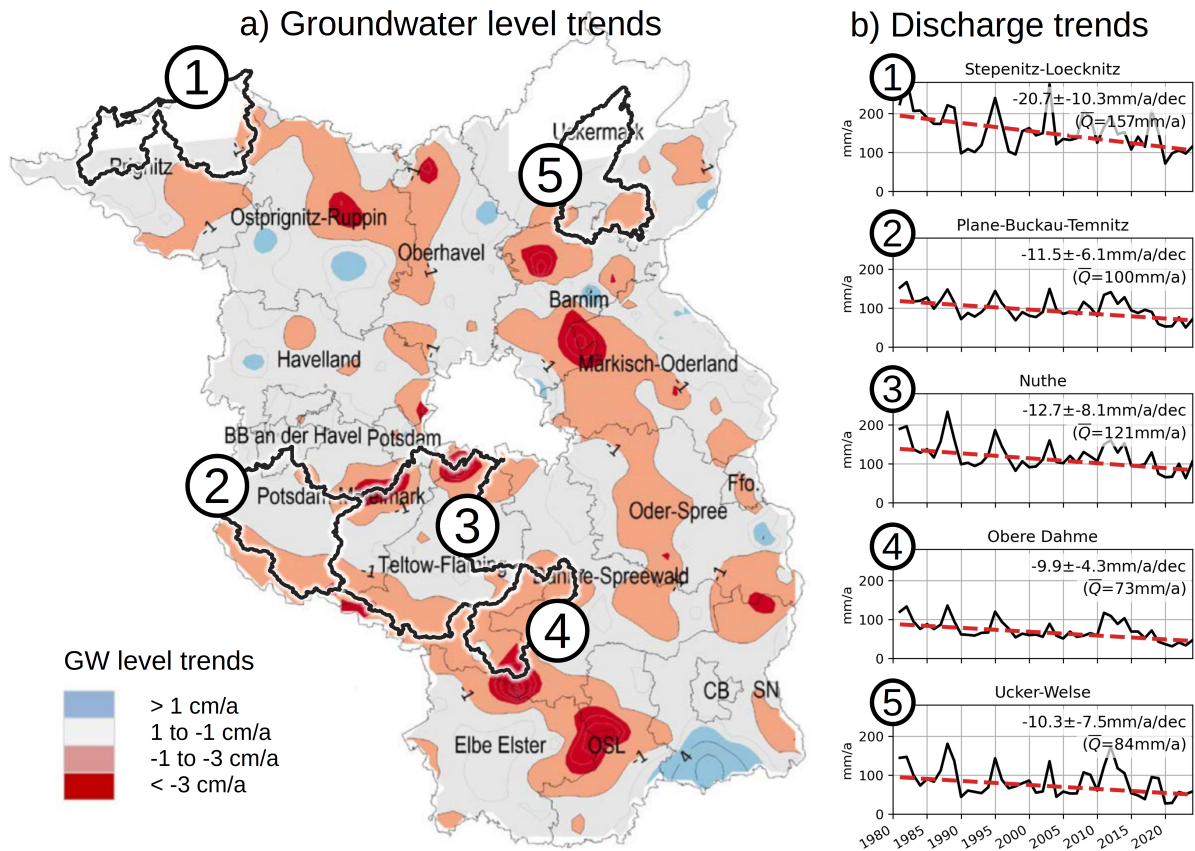


Figure 1. a) Interpolated trends of groundwater levels from linear regression at groundwater gauges in Brandenburg from 1976 to 2020, figure modified from Landesamt für Umwelt Brandenburg (2022) ([text in the map refer to county names](#)); b) Theil-Sen trends (all highly significant) of observed discharge (from 1980 to 2022) at selected river and stream gauges in Brandenburg that are largely unaffected by direct anthropogenic interference (see section 2.2 for details on the underlying data); [the unit of the trends \(\$\text{mm a}^{-1} \text{dec}^{-1}\$ \) corresponds to the change of discharge \(in \$\text{mm a}^{-1}\$ \) per time, i.e. decade \(dec\).](#)

elling study (Umweltbundesamt, 2024) that reports, for large parts of Brandenburg, only minor and mostly insignificant changes of GWR in the past decades (while Marx et al. (2024) even project increasing GWR in the future). In this context, our study aims to identify potential reasons behind such inconsistencies, or, in other words, to better understand which factors govern simulated GWR trends in Brandenburg over the past decades, and could hence explain the observed discharge trends.

65 For this purpose, we set up a range of simulation experiments to model GWR from 1980 until 2023 for the five aforementioned river basins in Brandenburg, and compare the corresponding simulated trends to observed discharge trends in these basins. To that end, we use a combination of model and data that is specifically tailored to the conditions in Brandenburg. In the following, we highlight specific aspects of this setup, and some of the underlying assumptions (details with regard to data and model will be described in sections 2 and 3, respectively):

70 – *Long-term trends in discharge are governed by GWR.* As already elaborated above, large parts of Brandenburg are dominated by permeable sandy soils. Hence, surface runoff is negligible (LUA Brandenburg, 2001), and river discharge is mainly fed from groundwater exfiltration. Any *long-term* trend in discharge can thus be interpreted as a long-term trend in GWR. The emphasis is on *long-term* (in the sense of multiple decades) ~~because any short-term dynamics~~, since we can assume that over long time periods, any GWR will also end up in the surface water bodies that drain the system.

75 Short-term dynamics of river discharge (e.g., across rainfall events or seasons, ~~might differ substantially~~) are, however, governed by the travel times of water along the different transit paths in the vadose zone and the aquifer. In contrast to discharge records, it is difficult to quantitatively infer representative GWR trends from time series of groundwater *levels* because of the uncertainty in the storage coefficient, the uncertain contribution of the upstream area to the observed level dynamics, the potential effects of local groundwater abstractions, and the limited spatial coverage of observation

80 points. Consequently, understanding of groundwater recharge dynamics from GW level data is hampered by inconsistent patterns, e.g., opposing trends (Lischeid et al., 2021).

– *The distance of the soil surface to the groundwater table is of utmost importance:* On the one hand, ~~close-shallow~~ groundwater tables in the lowland areas lead to very high evapotranspiration and hence to water budgets that are fundamentally different from areas with a deep groundwater table (LUA Brandenburg, 2001). The reason for this is the strong connectivity of the vegetation's root system to the ground water table. On the other hand, a ~~distant-deep~~ groundwater table (in Brandenburg up to more than 50 m) implies long transit times of the infiltrated water to the aquifer. Given the possibility of transit times in the order of years to decades, any change in the soil water balance might propagate quite slowly to the groundwater table. In order to capture all relevant processes across the entire unsaturated zone and range of transit times, we apply a physically-based 1-dimensional soil hydraulic model (SWAP, van Dam et al., 2008) in which we

85 conceive annual GWR as the net amount of percolation water that actually reaches the groundwater table after passing the entire unsaturated zone. Given the potentially long transit times of up to decades, our simulation already starts in 1951, even if we evaluate simulated GWR only from 1980 to 2023.

– *Long and homogeneous observational records of hydro-climatic variables are required in order to identify potential long-term trends in GWR.* In this context, it should be emphasized that climate change is not limited to global warming

95 (i.e. a temperature rise), but that other relevant climate variables might be subject to long-term trends, such as increasing solar irradiation ("global brightening", e.g., Wild, 2009), decreasing wind speed ("terrestrial stilling", e.g., Vautard et al., 2010) or trends in precipitation (in any direction). Unfortunately, the two criteria of "record length" and "homogeneity" can be considered as antagonistic in some instances: with the HYRAS dataset (Razafimaharo et al., 2020), the German Meteorological Service (Deutscher Wetterdienst, DWD hereafter) indeed provides a *long* record of daily grids

100 of important hydro-climatic variables from 1951 until 2020, based on interpolated gauge measurements. However, the underlying set of observational gauges can vary substantially over time, so that "trends in any one area may reflect the appearance and disappearance of specific stations, rather than the true local trend" (quoted from Hofstra et al., 2010). In our study, we hence decided to only use long-term observations from single climate stations instead of HYRAS data

(exceptions are documented in section 3.5) – being aware, of course, that these could be subject to inhomogeneities, too (e.g., due to changes in instruments, in measurement locations, or in the surroundings of the measurement locations Peterson et al., 1998). Only very few climate stations remain in Brandenburg which provide long daily records of the required climate variables (temperature, relative humidity and precipitation being the most complete; sun hours and wind speed being more problematic). In fact, we reduced our analysis to *four* climate stations (Potsdam, Lindenberg, Angermünde, Marnitz) with the most complete records between 1951 and 2023 and with the greatest proximity to our five study catchments. Only for precipitation, we extended this approach (further details with regard to the construction of homogeneous climate forcing data for our simulation model are provided in section 3.2).

– *The leaf area index (LAI) is a key vegetation parameter with potentially transient behaviour.* The LAI affects both transpiration and interception losses and has hence a fundamental impact on the actual evapotranspiration and, consequently, ~~ground-water~~ groundwater recharge. At the same time, there is strong evidence from remote sensing that the LAI has, in many regions of the world, significantly increased since the 1980s ("Earth's greening" Yang et al., 2023). In our study, we use a recently published LAI dataset (Cao et al., 2023) which spans from 1982 to 2020 in order to analyse the prevalence of such an LAI trend in Brandenburg as well as the potential effect on GWR trends.

In sections 2 and 3, we will give an overview of the data (namely discharge records, climatological data, landscape and vegetation attributes) and methods (namely the filling of gaps in climatological data, the soil hydraulic model, as well as the design of our simulation experiments). In section 4, we will present the GWR trends and their significance as resulting from our simulations, and discuss how these trends compare to the observed discharge trends. In section 5, we will comprehensively discuss limitations and uncertainties of our approach, and perspectives to address these in prospective research. In section 6, we highlight the implications of our study for both research and water resource management.

2 Data

2.1 Study area

Fig. 2 gives an overview of the study area and some of the underlying data. Brandenburg has a temperate continental climate characterized by cold winters and warm summers, and moderate precipitation that is evenly distributed throughout the year (mostly Cfb climate according to the classification of Koeppen and Geiger). Conditions are slightly drier in the east while maximum precipitation depths occur in the north west and in the south (see also Fig. 2).

The vast lowland areas of Brandenburg (mostly Urstromtäler from the Weichsel glacial period) are dominated by ~~close~~ shallow groundwater tables and hence high evapotranspiration rates, typically leading to a net water loss from these areas. Recharge of the groundwater mainly takes place in the more elevated areas, mostly consisting of moraines from the Weichsel epoch, except the south and west which are dominated by the Saale epoch. Soils are dominated by highly permeable sandy soils and loamy sands, as well as organic soils in the lowlands (LBGR, 2024).

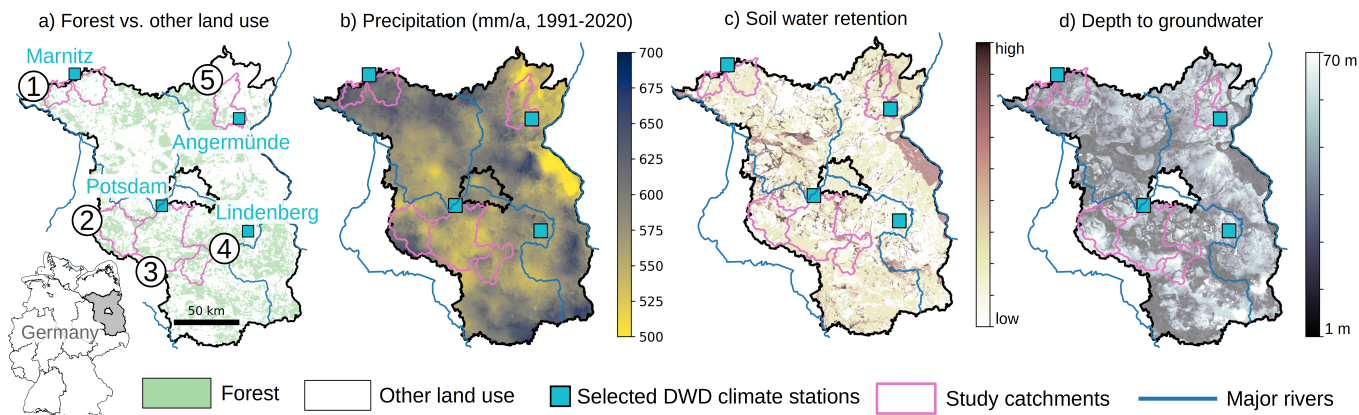


Figure 2. Overview of study catchments, selected DWD climate stations, and the spatial distribution of selected climate and landscape attributes: a) land use (forest versus other land use (i.e. mainly grass-/cropland, © OpenStreetMap contributors, 2024, distribution under ODbL license); b) average annual precipitation sum for the climate normal period 1991-2020, based on DWD’s HYRAS-DE-PR; c) top soil water retention capacity (LBGR, 2024); d) depth to the groundwater table (LfU, 2013).

135 The land use in Brandenburg is composed of 47.6% agriculture, 35.0% forests, 3.6% of other vegetated areas, 6.7% settlements, 3.5% traffic infrastructure, and 3.5% surface waters (Amt für Statistik Berlin-Brandenburg, 2023).

2.2 Discharge records

As river discharge in Brandenburg is governed by groundwater fluxes, we use long-term discharge observations as a reference for long-term changes in groundwater recharge (see section 1). Daily discharge observations are provided by the Brandenburg state environmental agency (Landesamt für Umwelt, referred to as LfU hereafter) via an online platform (Auskunftsplattform Wasser, <https://apw.brandenburg.de>).

The following criteria were applied to select discharge gauges for our analysis (see also section 1): (1) discharge records from at least 1980 to 2023; (2) a minimum upstream area of 500 km² to reduce the effect of uncertainties in the delineation of belowground watersheds; and (3) no major anthropogenic manipulation of the catchments water balance, e.g., by inter-basin water transfers or open pit mining (see section 1). ~~Neighbouring catchments were partly combined~~ In three cases, adjacent catchments were aggregated in order to further reduce the effect of uncertain belowground watersheds, and to increase the area over which the water balance is computed. ”Aggregating” two (or three) catchments means that their areas were merged to one coherent area, and that the observed runoff at the gauges of each catchment was summed up in order to obtain the total runoff from the merged area. Tab. 1 gives a comprehensive overview of the used discharge gauges and the ~~combination of upstream catchment areas~~ aggregation of catchment areas and runoff gauge observations for our analysis.

Table 1. Overview of selected discharge gauges in Brandenburg, and of combinations of catchments; trends are only computed for catchments or combinations larger than 500 km².

ID	Location name	River name	Catchment area (km ²)	Specific discharge (mm/a, 1980-2023)	Specific discharge trend (mm/a/dec, 1980-2023)
5871600	Potsdam	Nuthe	1792	121	-13
5861600	Märkisch-Bucholz	Obere Dahme	519	73	-10
5873600	Götting	Plane	465	-	-
5874601	Neue Mühle	Buckau	351	73	-
5874100	Brdb.-Wilhelmsdorf	Temnitz	132	-	-
	Combined	Plane-Buckau-Temnitz	948	100	-12
5935201	Wolfshagen	Stepenitz	570	168	-
5956000	Gadow	Löcknitz	465	143	-
	Combined	Stepenitz-Löcknitz	1035	157	-21
0491200	Prenzlau	Ucker	394	86	-
6950700	Schönermark	Welse	336	80	-
	Combined	Ucker-Welse	730	84	-10

2.3 Climate observations

Except for precipitation (see section 2.4), the hydro-climatological model forcing is entirely based on the climate station records (DWD, 2024a) provided by the German Weather Service (Deutscher Wetterdienst, DWD hereafter). Since the homogeneity of the forcing data is essential when analysing long-term GWR trends, we did not use gridded products (such as HYRAS-DE) which are based on interpolation (Hofstra et al., 2010, see also section 1 for more explanation).

Instead, we identified four DWD climate stations in Brandenburg that are (1) close to the selected study catchments, and that (2) show a fairly complete record of required daily climate variables over the time period from 1951 until 2023: Potsdam, Lindenberg, Angermünde, and Marnitz. These stations are highlighted in Fig. 2. The climate variables required from these stations include: daily solar irradiance (kJ/m²/d), precipitation (mm/d), daily minimum and maximum temperature (°C), relative humidity (%), [wind speed \(m/s\)](#), and daily sunshine hours (h/d, required in case solar irradiance is unavailable, see section 3.2).

Still, not all required climate variables were recorded at all stations, and some stations still exhibit data gaps. In section 3.2, we document how we filled the data gaps for different climate variables and stations while attempting to maintain homogeneity of the time series as best as possible.

2.4 Precipitation observations

Long-term precipitation trends are much less coherent across Brandenburg than trends for other climate variables. In addition, more precipitation stations exist than climate stations. Therefore we decided to evaluate the effect of different precipitation

forcings on the trends of simulated GWR. For that purpose, we included the following precipitation times series in addition to those observed at the four climate stations:

- Observations from other precipitation gauges (DWD, 2024b) within a 5 km buffer around each study catchment: since there is a trade-off between the number of available station records versus the length and completeness and hence the homogeneity of these records, we decided to apply the following filtering criteria: we used only station stations with less than a total of 1 % missing data between 1980 and 2023, and less than 5 % missing data for individual years between 1980 and 2023. We also included gauges with records that do not fully reach back until 1951. These will be specifically marked in the results since the corresponding GWR simulation will not have a fully homogeneous forcing during model spin-up). Based on these criteria, we obtained between 0 and 7 additional precipitation records for each study catchment (see Tab. 3).
- We already pointed out that using gridded hydro-meteorological interpolation products is prone to introduce artificial local trends, specifically in a setting in which many precipitation gauges were introduced between 1960 and 1980, but also discontinued after 1990. Still, we investigate the effect of one such product (HYRAS-DE-PR, DWD, 2024c), simply because this is the most prominent regionalised precipitation product for climate impact studies in Germany. For that purpose, we use the daily areal average of HYRAS-DE-PR across the selected study catchments from 1951 to 2023.

2.5 Leaf area index and other vegetation parameters

In order to correctly capture magnitude and seasonality of forest LAI, we used data from Level II plot collections of the UNECE Convention on Long-range Transboundary Air Pollution (ICP Forests), which comprise eight forest sites for Brandenburg, five of which monitor Scots pine (*Pinus sylvestris*) forests which represent 70 % of the state's forests. The data on these five sites reaches back to 2016. On this basis, we constructed the average seasonal LAI development for this species. A similar procedure was applied to construct the average seasonal progression of LAI for grassland and cropland, based on typical crop representations for Central Europe in the SWAP model library (Kroes et al., 2017).

In order to quantify and consider potential long-term trends in LAI, we used a dataset of global LAI estimates from 1982 to 2020 that was recently published by Cao et al. (2023). The aim of this dataset is specifically to maximise spatiotemporal consistency. For this purpose, various satellite-based NDVI and LAI products as well as millions of field LAI measurements were fused by means of a back propagation neural network. The spatio-temporal resolution of the dataset is 1/12 degree (about 5 km in Brandenburg) and approximately two weeks. For our study, we extracted the data for Brandenburg and computed, for each time step, the areal average LAI for the entire state (in order to get a more robust signal in comparison to computing areal average values only for the selected catchments). For the resulting time series of biweekly LAI values from 1982 to 2020, we computed a Theil-Sen trend which amounted to an increase of $0.1 \text{ m}^2 \text{ m}^{-2}$ per decade. This trend was superimposed on the aforementioned seasonal LAI developments for forest and grassland in the SWAP model (see also section 3.4, and section 5.3 for a discussion of the limitations of this approach).

2.6 Other geodata

200 In order to categorize the landscape, within each considered river basin, into similar functional units (hydrotopes), we used the following data sources for land use, soil, and the distance to the groundwater table:

- **Land use:** to delineate forests from grassland and cropland, we used the land use layer from OpenStreetMap (OpenStreetMap contributors, 2024).
- **Soil data:** We used the BUEK300 soil map (LBGR, 2024) in order to obtain the dominant soil type per study catchment
205 (medium sand for all catchments except Ucker-Welse and Stepenitz-Löcknitz, for which the dominant soil is loamy sand) and the corresponding dominant soil texture which is required as an input to a pedotransfer function to determine the soil hydraulic parameters of the simulation model (see section 3.4).
- **Depth to the groundwater table:** To represent the depth of the groundwater table and hence the lower boundary condition for the soil hydraulic model, we used a dataset provided by the Brandenburg Landesamt für Umwelt (LfU, environmental state agency) which represents the depth of the unsaturated zone as obtained from a combination of a
210 digital elevation model and groundwater level contours constructed by means of interpolation (LfU, 2013). [The dataset provides the mid points of depth classes, corresponding to a finite number of 13 depth classes \(1, 2, 3, 4, 5, 7.5, 10, 15, 20, 30, 40, 50, and 70 m\). The depth resolution is higher \(meter-resolution\) for shallow groundwater tables which is particularly important for modelling the water balance \(section 3.4\), since the groundwater depth has a strong influence on evapotranspiration when the groundwater table is shallow \(see section 1\).](#)
215

3 Methods

3.1 [Methodological overview](#)

[The main methodological approach of our study is to simulate series of GWR in each study catchment for the period from 1980 to 2023. From these series, we computed the trends in GWR and compared them to the corresponding trends of observed discharge. A good agreement between both would indicate that the simulation model is able to explain the discharge trends as outlined in Fig. 1 and Tab. 1 \(see also section 1 for additional background\).](#)
220

[To obtain GWR, the one-dimensional Soil-Water-Atmosphere-Plant model \(SWAP, van Dam et al., 2008, section 3.4\) was used to simulate the surface water balance and the resulting percolation of water through the unsaturated zone down to the groundwater table. This daily "bottom flux" was aggregated to obtain the annual sum of groundwater recharge.](#)

225 [In order to obtain the spatial average of GWR per catchment, we followed the concept of "hydrotopes", i.e. spatial sub-units that are considered as homogeneous with regard to \(i\) climate forcing, \(ii\) soil texture, \(iii\) land use, and \(iv\) groundwater depth. For each catchment, climate and soil were assumed to be uniform across the entire catchment \(i.e. one class each per catchment\): the climate forcing was based on the nearest of the four selected climate stations \(section 2.3\), and soil texture was represented by the dominant soil texture class in the catchment \(section 2.6\). Land use and groundwater depth, however,](#)

230 were assumed to be heterogeneous across the catchment: land use was represented by two classes (forest and grass-/cropland) and groundwater depth by 13 classes (see section 2.6). This resulted into a total of 26 hydrotope classes (1 climate x 1 soil x 2 land uses x 13 groundwater depths). By spatially intersecting all four layers, we quantified the areal fraction of each hydrotope class per catchment. Running the SWAP model for each of the 26 hydrotope classes, the daily GWR per catchment was then obtained as the area-weighted average of the simulated daily bottom flux per hydrotope.

235 In the following subsections, we further explain the treatment of missing hydro-climatological data (section 3.2), the precipitation correction (section 3.3), the SWAP model and its parameterisation (section 3.4), the specific design of the simulation experiments (section 3.5) and the calculation of trends (section 3.6).

3.2 Filling missing data for solar irradiation and wind speed

For Potsdam, Lindenberg, Angermünde and Marnitz, the percentage of missing data between 1951 and 2023 is below 0.1 %
240 for each of the variables daily minimum/maximum temperature, relative humidity, and precipitation depth. For solar irradiation and wind speed, though, only Potsdam has an almost complete record (less than 1% missing data). Records of solar irradiation in Lindenberg only started in 1980 and have considerable gaps between 1997 and 2001 (while wind speed at Lindenberg has less than 1% missing data). Angermünde and Marnitz have no records of solar irradiation, and measurements of wind speed only started around 1980. Furthermore, many wind speed measurements across Brandenburg are affected by strong
245 inhomogeneities, mainly because the measurement height varied over time. In the following, we outline our approach to provide fairly homogeneous time series for solar irradiation and wind speed as our model forcing.

Solar irradiance is a key input to the computation of evapotranspiration using the ~~Penman-Monteith~~ Penman-Monteith method; however, Potsdam is the only climate station in the state with a comprehensive record from 1951 to 2023. Lindenberg, in turn, has an almost complete record of daily sunshine hours. Using the observations of solar irradiance and sunshine hours in
250 Potsdam, we trained a random forest (100 trees and a maximum node depth of 10) to model solar irradiance from the following predictive features: clear-sky radiation as simulated from geographic coordinates, altitude, and datetime by the Python package pvlib (~~Holmgren et al., 2018; Anderson et al., 2024~~) (Holmgren et al., 2018; Anderson et al., 2024, using the function "get_clearsky" and a
, sunshine hours per day, relative and absolute humidity, and seconds elapsed since ~~1951 (with 1951~~. The resulting random forest model yielded an R^2 of 98.4 % on independent test data, ~~and with~~ clear-sky radiation and sunshine hours being the most
255 important features by far). We used this random forest model to fill the data gaps for solar irradiance at Lindenberg. For the climate stations in Angermünde and Marnitz, however, the record of sunshine hours between 1951 and 2023 had too many gaps. In order to ensure a homogeneous record of sunshine hours as an input to the random forest, we used the sunshine data from Potsdam and applied a multiplicative scaling factor to adapt it to the average conditions in Angermünde and Marnitz. This factor was obtained from the ratio of the mean values at both stations (Potsdam and Angermünde or Marnitz, respectively) for
260 those periods in which both stations had data. With these complete records of sunshine hours, the aforementioned random forest model was applied to Angermünde and Marnitz in order to obtain solar irradiance.

Wind speed Wind speed is observed at 23 DWD stations in Brandenburg. At only seven of these, the sensor measures at 10 m above ground - a reference height commonly used in precipitation correction and for calculating evapotranspiration. With

record lengths of 10–52 years, none of these stations covered the entire study period (1951–2023). Conversely, ERA5-Land
265 (Muñoz Sabater et al., 2021) offers hourly values for wind speed at approximately 9 km resolution. However, ERA5-Land only
showed poor agreement with observed trends and magnitudes. In order to obtain continuous wind speed records at the seven
aforementioned stations, we trained a random forest model ([100 trees, maximum node depth of 10](#)) at each of these stations
by using the available [daily](#) wind speed observations at 10 m as training data. As predictive features, we used the local [daily](#)
ERA5-Land wind speed estimates and the wind speed observed at the climate station in Potsdam. R^2 values ranged from 0.74–
270 0.89 on independent test data. These random forest models served for reconstructing daily wind speed at the seven stations for
the full study period. For Potsdam, Lindenberg, Angermünde and Marnitz, we then used the reconstructed wind speed at the
nearest of these seven wind stations.

3.3 Precipitation correction

Standard precipitation gauges experience considerable undercatch, mainly due to wind-induced turbulence. To account for the
275 effects on rain and snow, we used the correction according to Kochendorfer et al. (2017) for unshielded gauges which requires
wind speed at 10 m (see section 3.2) and air temperature at 2 m. It should be emphasized that this correction method could
affect the trend of the corrected precipitation in case the underlying wind speed records show a trend. This is, however, an
intended behaviour because a change in wind speed at the gauge location also changes the corresponding measurement error
that needs to be corrected for. To assess this effect, we also analysed the uncorrected precipitation and the standard correction
280 used by DWD (Richter, 1995), which uses fixed monthly coefficients for geographic regions and station exposure (codes C and
d, according to Richter, 1995).

3.4 Soil hydraulic model

The Soil-Water-Atmosphere-Plant (SWAP, van Dam et al., 2008) model was employed to simulate soil water dynamics and
groundwater recharge within the study area. This 1D-model calculates vertical soil water movement by solving the Richards
285 equation, which accounts for infiltration and capillary rise, based on soil hydraulic properties and governing boundary condi-
tions. Evapotranspiration [depends on atmospheric conditions as well as on vegetation and soil properties and](#) is estimated using
the Penman-Monteith equation, ~~integrating factors such as soil moisture content, vegetation type, and atmospheric conditions.~~
~~This in combination with the Feddes model which accounts for the limitation of transpiration by the availability of soil water~~
[\(Kroes et al., 2017\). The](#) dual focus on soil hydrology and atmospheric interactions allows for a detailed analysis of the surface
290 water balance and the percolation of water through the unsaturated zone down to the groundwater table. This "bottom flux" is
considered as the groundwater recharge (which can also be negative in case of a net flux from the groundwater table to the sur-
face, typically in the case of areas with shallow groundwater tables during the summer). For our model setup, the groundwater
table depth was considered as static (corresponding to a Dirichlet boundary condition, see also section 2.6).

Tab. 2 highlights important vegetation-related model parameters that were used for our study. Furthermore, soil hydraulic
295 parameters (SHP) need to be set in order to represent the relationships between matrix potential (ψ , hPa) and volumetric soil
water content (SWC, m^3/m^3) as well as hydraulic conductivity (K_s , m/d). Using to the model of van Genuchten and Mualem

(van Genuchten, 1980), the SHP correspond to five parameters: residual water content (θ_r , m^3/m^3), saturated water content (θ_s , m^3/m^3), air entry point (α , m^{-1}), and the shape parameter of the retention curve (n , dimensionless). The values of these parameters were set based on the widely used pedotransfer function ROSETTA (Schaap et al., 2001) which requires soil texture and soil bulk density as input. These soil parameters were obtained from the soil map BUEK300 for the dominant soil in each study catchment (see also section 2.6). Altdorff et al. (2024) have recently shown that the same model implementation and parameterisation could well reproduce soil water dynamics across eight monitoring locations in Brandenburg (covering major land use and soil types as well as different groundwater table depths).

Table 2. Overview of key SWAP model parameters related to vegetation and corresponding references.

Parameter name	Meaning	Forest	Grass/cropland	References
Leaves and roots				
GCTB	Max. leaf area index (LAI) [-]	3.5	3.0	See sect. 2.5
RDTB	Rooting depth [cm]	150	40	Guerrero-Ramírez et al. (2021)
Evapotranspiration				
RSC	Minimum canopy resistance [s/m]	180	130	Guan and Wilson (2009)
Interception acc. to...				
...Von Hoyningen-Huene (1983)				
COFAB	Interception coefficient [cm]	-	0.25	Kroes et al. (2017)
...Gash et al. (1995)				
PFREE	Free throughfall coefficient [-]	0.32	-	Russ et al. (2016)
PSTEM	Stem flow coefficient [-]	0.02	-	
SCANOPY	Storage capacity of canopy [cm]	0.08	-	
AVPREC	Avg. rainfall intensity [cm/d]	3.30	-	
AVEVAP	Avg. evaporation int. during rain [cm/d]	0.46	-	

3.5 Retrieving the average modelled GWR per catchment

For each catchment, we defined hydrotopes by intersecting the dominant soil type in that catchment, the land use (forest versus grass-/cropland), the classes of groundwater depth (1, 2, 3, 4, 5, 7.5, 10, 15, 20, 30, 40, 50, and 70 m, as provided by LfU, 2013) and the nearest of the four selected climate stations. For each hydrotope, we simulated the daily bottom flux from 1951 to 2023. For very deep soil columns, the model requires a considerable spin-up period to eliminate the influence of its initial conditions. This spin-up period corresponds to the transit time of water from the surface to the groundwater, and can correspond to several decades. We therefore only evaluated the bottom flux data with beginning of 1980.

For each daily simulation time step, we obtained the average groundwater recharge per catchment by an area-weighted average of the simulated bottom flux. The weights result from the areal proportion of each hydrotope category in the catchment. For analysis, we aggregated the daily values to annual cumulative amounts of GWR per hydrotope and catchment.

3.5 Design of simulation experiments

315 The hydro-climatic model forcing includes daily values for solar irradiation, temperature, humidity, wind speed, and precipitation. Except for precipitation, this forcing was obtained for each study catchment by assigning the observations (or reconstructed observations, see section 3.2) of one of the four selected climate stations (see Tab. 3). Due to the importance of precipitation for GWR and the large uncertainty of precipitation trends (due to high inter-annual variability), we tested a larger set of precipitation time series as model forcing for each study catchment:

- 320
- the precipitation observed at the selected climate station
 - synthetic trends: we removed the trend from the observed precipitation at the selected climate station and then imprinted different linear trends, ranging from -20 to $+20 \text{ mm a}^{-1} \text{ dec}^{-1}$ in increments of $2 \text{ mm a}^{-1} \text{ dec}^{-1}$.
 - precipitation observed at other precipitation gauges (individually, i.e. without any further weighting) in or close to the study catchments (ref. section 2.4).
- 325
- the areal average of precipitation in the study catchment as obtained from the gridded HYRAS-DE-PR dataset (ref. section 2.4).

In combination with the two LAI scenarios (static versus transient), this resulted in a total number of 262 realisations (see Tab. 3).

3.6 Trend calculation

330 All trends in this paper were calculated using Theil-Sen estimates (Theil, 1950; Sen, 1968) to compute the slope of the trend. This method is commonly used in hydrometeorological analyses (see, e.g., Yue et al., 2002), more robust to outliers and independent of the assumption of normally-distributed residuals, while otherwise producing results similar to linear regression. All trends are reported with reference to a 10-year-period, denoted as decade or "dec" hereafter. The significance of the trends is likewise computed according to Sen (1968), and expressed as the p-value.

335 4 Results and Discussion

4.1 Trends in hydro-climatic model forcing

Fig. 3 summarizes the hydro-climatological model forcing at the four selected DWD climate stations in Brandenburg: Potsdam, Lindenberg, Marnitz and Angermünde. The potential evapotranspiration (ET_P , computed using the Penman-Monteith method according to Kroes et al., 2017) shows a highly significant positive trend across all four stations (similar for all stations, but
340 highest at Lindenberg). ET_P integrates the effects of other climate variables, namely solar irradiation and air temperature which increase at all stations (causing the effective increase in ET_P), and wind speed which decreases at all stations (counteracting the increase of ET_P).

Table 3. Overview of simulation experiments [and input data used](#). The [first two last](#) column headers refer to [explains](#) the [standard abbreviations for hydro](#) of resulting realisations as the [surface: minimum and maximum air temperature at 2 m](#), [product of the number of precipitation](#) ([tasmin](#), [tasmax](#), [third column](#)), [the number of LAI input variants](#) ([hurs](#), [forth column](#)), [solar irradiation](#) ([rsds](#)), [wind speed at 10 m](#) ([sfeWind](#)), [precipitation](#) ([pr](#)). The entries in column "pr" are [DWD's unique station identifiers](#).

Catchment	tasmin , tasmax , hurs Main meteo input ¹ rsds , sfeWind (misc.)	pr Precipitation (mm)	LAI trend ($\text{m}^2\text{m}^{-2}\text{a}^{-1}\text{dec}^{-1}$)
Stepenitz- Löcknitz	Marnitz	Marnitz	0.0 or +0.1
		Synthetic trend [-20,-18, ..., 20 mm a ⁻¹ dec ⁻¹]	0.0 or +0.1
		pr-gauges DWD IDs ² : 2779	0.0 or +0.1
		HYRAS-DE-PR areal average	0.0 or +0.1
Plane- Buckau- Temnitz	Potsdam	Potsdam	0.0 or +0.1
		Synthetic trend [-20,-18, ..., 20 mm a ⁻¹ dec ⁻¹]	0.0 or +0.1
		pr-gauges DWD IDs ² : none	0.0 or +0.1
		HYRAS-DE-PR areal average	0.0 or +0.1
Nuthe	Potsdam	Potsdam	0.0 or +0.1
		Synthetic trend [-20,-18, ..., 20 mm a ⁻¹ dec ⁻¹]	0.0 or +0.1
		pr-gauges DWD IDs ² : 3915, 5092, 427, 2863, 3124, 4108, 5555	0.0 or +0.1
		HYRAS-DE-PR areal average	0.0 or +0.1
Obere Dahme	Lindenberg	Lindenberg	0.0 or +0.1
		Synthetic trend [-20,-18, ..., 20 mm a ⁻¹ dec ⁻¹]	0.0 or +0.1
		pr-gauges DWD IDs ² : 3915	0.0 or +0.1
		HYRAS-DE-PR areal average	0.0 or +0.1
Ucker-Welse	Angermünde	Angermünde	0.0 or +0.1
		Synthetic trend [-20,-18, ..., 20 mm a ⁻¹ dec ⁻¹]	0.0 or +0.1
		pr-gauges DWD IDs ² : 3995, 5899	0.0 or +0.1
		HYRAS-DE-PR areal average	0.0 or +0.1

¹ [daily minimum and maximum air temperature at 2 m, relative humidity at 2 m, solar irradiation, and wind speed at 10 m](#)

² [IDs of DWD's precipitation gauges which were used as alternative precipitation forcing \(see section 3.5\)](#)

While it is obvious that any trend in ET_P will not directly translate to actual evapotranspiration (which is constrained by actual soil water availability), ET_P represents a forcing component that consistently acts towards an increase in actual evapotranspiration and hence a decrease in GWR across all stations.

As for precipitation, the four climate stations feature negative trends at Potsdam, Lindenberg and Marnitz (all at similar rates), and a positive trend at Angermünde. However, none of these trends are significant. The situation is similar if we include other precipitation gauges in Brandenburg (Fig. 4): looking only at gauges with complete records, opposite trend directions exist across the state between 1980 and 2023, ranging roughly between -20 and +20 mm a⁻¹ decade⁻¹.

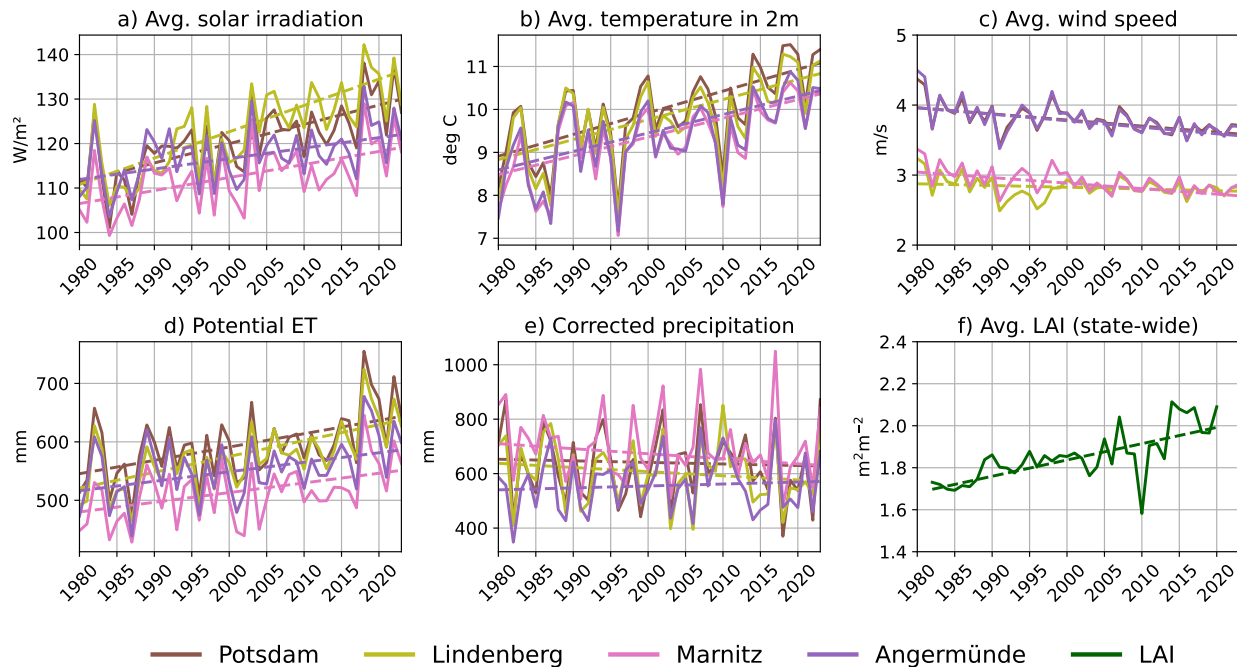


Figure 3. Aggregate annual values of selected climate variables at DWD’s climate stations Potsdam, Lindenberg, Marnitz, and Angermünde from 1980 to 2023, and LAI as obtained from Cao et al. (2023) (only available from 1982 to 2020): a) solar irradiation (annual average), b) air temperature at 2 m (annual average), c) wind speed (annual average), d) reference evapotranspiration (annual sum), e) precipitation (corrected acc. to Kochendorfer et al., 2017, annual sum), f) Brandenburg-wide average LAI (annual average). Dashed lines show Theil-Sen trend slopes which are all highly significant except for precipitation for which *none* of the trends is significant; note that series for solar irradiation and wind speed were partly reconstructed (see section 3.2), potential ET was computed using the SWAP model.

350 Precipitation correction (see [Seet. section 3.3](#)) not only corrects the total amount (i.e. +4–6 mm/a for Kochendorfer et al. (2017), +9–10 mm/a for Richter (1995)), but may also affect the trends: Kochendorfer et al. (2017) reinforces the negative trends by up to $-4 \text{ mm a}^{-1} \text{ decade}^{-1}$ while Richter (1995) shows a minor amplification of positive trends (results not shown).

Again, none of these trends is significant, but even insignificant precipitation trends might affect trends in simulated GWR. The simulation experiment covers various combinations of precipitation series for each catchment in order to investigate the
 355 relevance of this effect.

4.2 Trends in GWR

Fig. 6 shows the trends in GWR-5 shows annual series of simulated GWR (solid blue lines). As examples from the simulations experiments in Tab. 3, we chose the ones in which the model was forced by the observations from the four selected climate stations (including precipitation), together with the specified LAI trend of $0.1 \text{ m}^2 \text{ m}^{-2}$. In comparison to the annual series
 360 of observed river discharge (solid black lines), we find that the interannual variability and the average water balance match

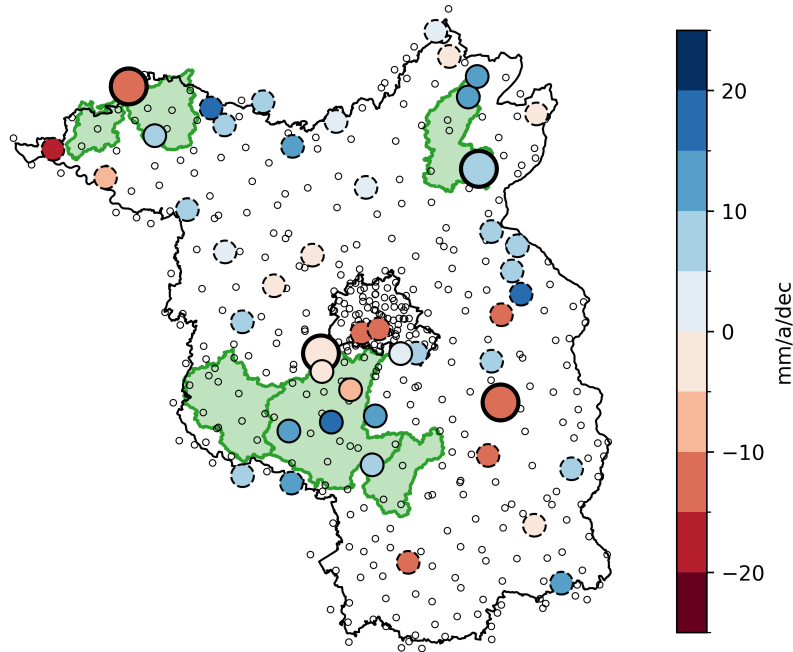


Figure 4. Precipitation trends between 1980 and 2023: the small hollow dots show all daily precipitation gauge locations in DWD's collection; the coloured dots show the trend at gauge locations with complete records at least between 1980 and 2023 (large dots: trend at the four selected climate stations Potsdam, Lindenberg, Marnitz, Angermünde; dots with solid circles: precipitation gauges within the catchments, see Tab. 3; dots with dashed borders: other gauges with complete records). Note that none of the shown trends is significant at the 5% level.

fairly well, with some overestimation in the Stepenitz-Löcknitz and some underestimation in the Nuthe catchment. In general, the response of the river discharge is more dampened which is plausible as it also includes the transit of water through the aquifer, which is not considered in our model. More importantly for our study, the long-term trends of observed discharge and simulated GWR correspond quite well - except for the Ucker-Welse catchment where the modeled trend is much weaker than the observed one.

365

In order to put the trend examples from Fig. 5 into a more comprehensive context, Fig. 6 shows the simulated GWR trends as they result from ~~the simulation experiments outlined in section 3.5.~~ all simulation experiments in Tab. 3.

370

In each catchment, the model forcing is based on the observations of one of the four selected climate stations - except for the variables precipitation and LAI. As summarized in Tab. 3, each model run within a given catchment represents the combination of a specific LAI forcing ("static LAI" or "transient LAI", see Fig. 3f) with one precipitation forcing (which in turn is characterised by a specific trend). Each point in the figure hence marks the combination of an LAI trend (blue/red colour), a precipitation trend (abscissa), and the resulting GWR trend (ordinate). Precipitation time series were obtained from the selected climate stations (large triangles), from additional precipitation gauges within the catchments (small triangles),

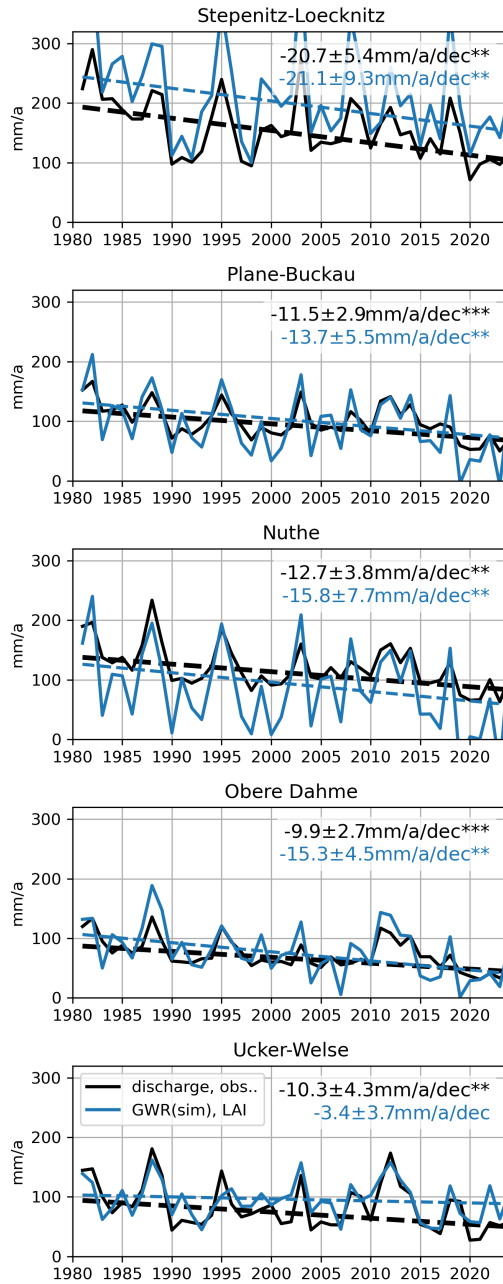


Figure 5. Annual observed river discharge and modelled groundwater recharge (1980 - 2023), driven by the selected climate stations, including the trend in LAI. The dashed lines illustrate the fitted trend, the (coloured) numbers specify the corresponding trend magnitudes, their 95%-confidence intervals and the significance levels (***) $p < 0.001$; **) $p < 0.05$; *) $p < 0.1$.

from the gridded HYRAS-DE-PR dataset (squares) and from artificial series with superimposed trends (dots and lines). The fill colour of the markers illustrates the significance level of the resulting GWR trend. The green horizontal line represents the mean and the green shade the 95% confidence interval (CI) of the observed discharge trends for each catchment. In order to understand how to relate Fig. 6 to the previous Fig. 5, just note that the large blue triangles in Fig. 6 represent the same GWR trends as the blue lines in Fig. 5.

Altogether, the figure should help us to disentangle the effects of precipitation and LAI trends on simulated GWR trends, and to evaluate how well the simulated GWR trends correspond to the trends in observed discharge (which, in the long run, should correspond to the actual trends in GWR). Along these lines, Fig. 6 allows the following observations:

- Negative precipitation trends act towards negative GWR trends (and the same, of course, in the opposite direction). As such, this qualitative statement may appear self-evident. Yet, the strength of this relationship, together with the wide range of observed precipitation trends (even though not significant), was surprising to us.
- There is a substantial offset between the blue ("transient LAI") and red ("static LAI") markers in the order of -3 to $-5 \text{ mm a}^{-1} \text{ dec}^{-1}$, meaning that the LAI trend causes GWR trends to be more negative (in comparison to using the same seasonal LAI dynamics each year). Given that the LAI trend of $0.1 \text{ m}^2 \text{ m}^{-2} \text{ a}^{-1} \text{ dec}^{-1}$ is highly significant and retrieved from observations, we consider the corresponding simulations (blue markers and lines) as more representative for the situation in the selected catchments than the red markers, and will hence focus the following discussion on the blue markers.
- Our key question is whether the observations of climate variables and LAI produce simulated GWR trends that are consistent with the trends in observed discharge, in other words: do the resulting GWR trends fall within the 95 % CI of the observed discharge trend (green shade) *and* are they significant? First, we take a look at our prime hydro-climatological forcing data – the selected climate stations: all large blue triangles fall within the 95 %-CI and are significant (except for the Ucker-Welse catchment where the GWR trend is not significant). This strongly supports the hypothesis that the past climate and LAI trends *together* explain the observed decline in discharge.
- The situation becomes less coherent if we use the precipitation from HYRAS-DE-PR instead: while the large blue squares fall into the green interval for all catchments except the Plane-Buckau-Temnitz, the corresponding GWR trend is ~~significant at~~ at least significant at a level of $p=0.1$ in (corresponding to all dots in Fig. 6 except those with the lightest shade of grey) in only one out the five cases (, i.e. for the Obere Dahme).
- Considering additional precipitation gauges from the catchment as alternative model forcing further complicates the picture: for the Stepenitz-Loecknitz catchment, the one additional gauge falls out of the 95 %-CI; for the Plane-Buckau-Temnitz, there is no additional gauge; for the Nuthe, three out of seven additional gauges fall out of the 95 %-CI; for the Obere Dahme, the one additional gauge falls into the 95 %-CI; and for the Ucker-Welse, the two additional gauges fall out of the 95 %-CI.

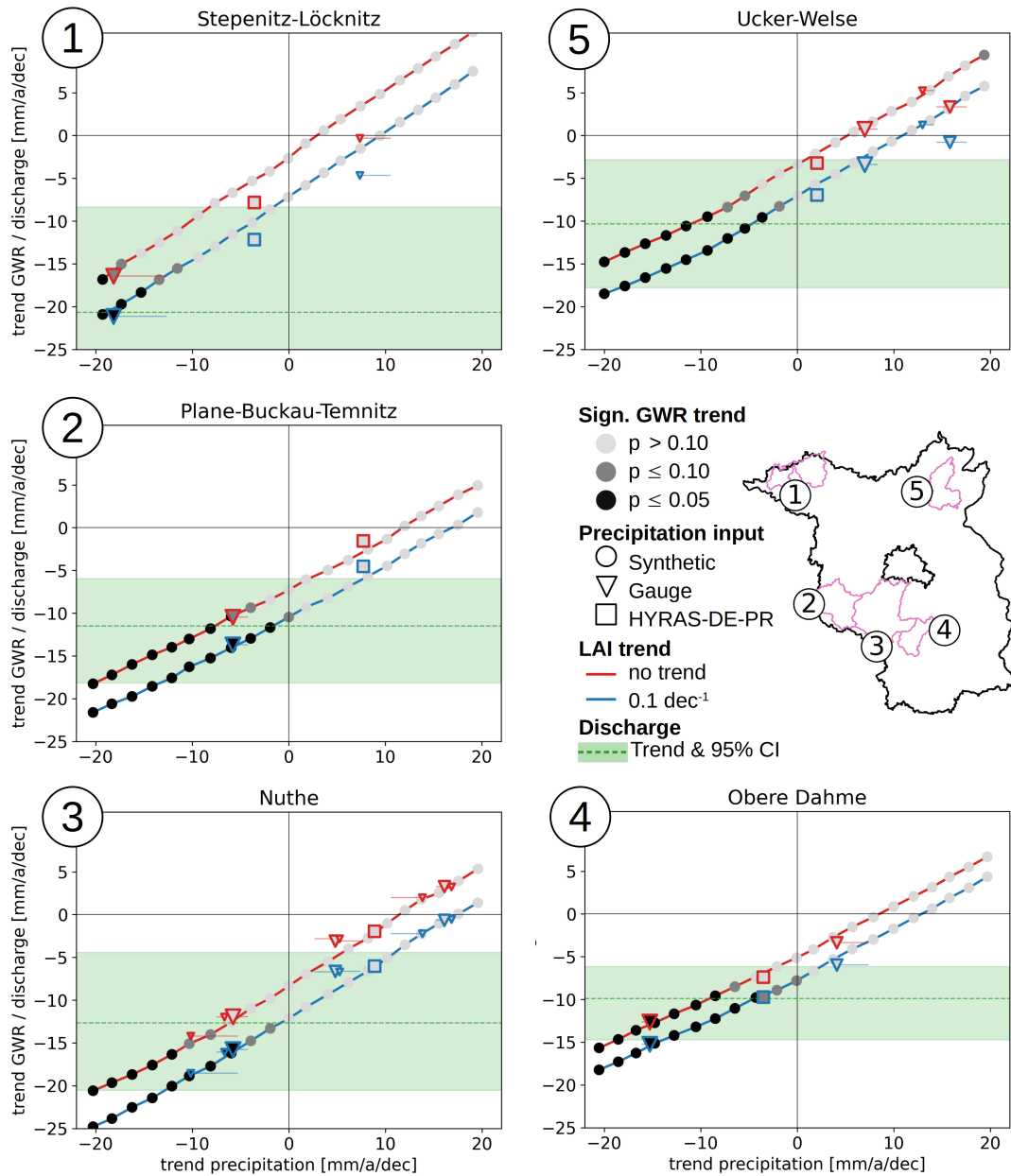


Figure 6. Effect of precipitation and LAI trends on GWR trends (1980-2023). Blue/red: with or without transient LAI trend; circles/lines: response to synthetic precipitation with superimposed trend; triangles: response to precipitation observed at selected gauges (large: selected climate station, medium/small: other rain gauges within catchment complete since 1951/1980), corrected acc. to Kochendorfer et al. (2017); associated whiskers display range of rainfall corrections (uncorrected, Richter (1995), and Kochendorfer et al. (2017)).

- 410
- In four cases, the GWR trend as inferred from HYRAS-DE-PR (squares) falls inbetween the trends inferred from rain gauges (triangles). ~~While this is plausible~~This is plausible. Still, trends from HYRAS-DE-PR ~~still~~ need to be considered with care (as repeatedly mentioned before) because they are based on temporally varying sets of gauges – which could result in trend artefacts. This may apply in the Ucker-Welse catchment where the trend in HYRAS-DE-PR precipitation is smaller than the trend of any of the shown rain gauges.
 - The majority of blue markers with sufficiently long records (11 out of 14 triangles and squares) fall inside the 95 %-CI of observed discharge trends; yet, there appears to be a general gap in the sense of simulated GWR trends underestimating the magnitude of the observed negative discharge trends, or even being positive.
 - 415 – It should be noted that none of the observed precipitation trends are significant. Still, GWR trends can be significant even when the trend in precipitation forcing is not - depending on the trend in evaporative forcing.
 - The use of artificially imposed precipitation trends helps us to generalize the results beyond the observed precipitation trends: triangles and squares align mostly well along the blue and red lines that result from the use of precipitation series with artificial trends. This underlines, for the present context, the dominant effect of trends in annual precipitation on GWR trends (in comparison to other specific rainfall characteristics at the stations such as event properties or
420 seasonality).
 - The ~~offsets of~~intercepts (ordinate value at an abscissa value of 0) of the blue lines indicate that the GWR trend is always negative if the precipitation trend is zero. Except for the Stepenitz-Löcknitz catchment, all these GWR trends at a zero precipitation trend fall into the 95 %-CI of the observed discharge trend *and* are significant. This is an important aspect, given that the median of all precipitation trends shown in Fig. 4 is close to zero. GWR trends keep falling into the 95 %-
425 CI of the observed discharge trend even for positive precipitation trends of up to $10 \text{ mm a}^{-1} \text{ dec}^{-1}$ (Nuthe), albeit not being significant anymore.
 - The slope of the red/blue lines are slightly steeper for higher precipitation trends and for the Stepenitz-Löcknitz catchment, suggesting a more direct response of GWR to precipitation under more humid conditions.
 - Finally, it should be noted that, for some stations, the horizontal whiskers show a considerable influence of the rainfall
430 correction on the resulting trend, which can comprise several $\text{mm a}^{-1} \text{ dec}^{-1}$.

How to sum up the results from the admittedly complex Fig. 6? Based on the four selected climate stations, we consider it very likely that the decreasing discharge trends in the five catchments were caused by the combination of climate change and increasing LAI; based on the alternative precipitation forcings (HYRAS, other gauges), this is still to be considered likely, albeit at lower confidence. But even though the majority of precipitation series effectuates GWR trends that are negative and
435 coincide with the 95 %-CI of the observed discharge trends, these GWR trends are, in most cases, less negative compared to the observed negative discharge trend. Potential causes for this apparent gap are discussed in section 5.

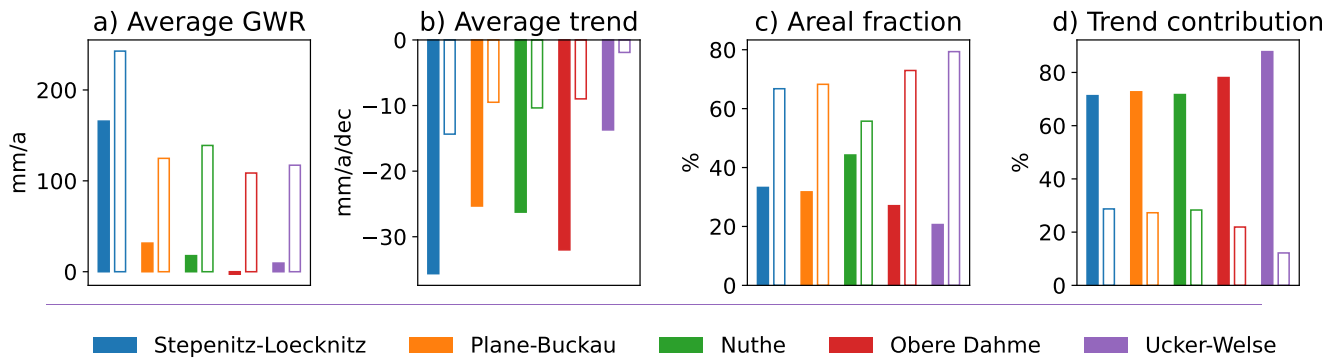


Figure 7. Influence of groundwater depth on average values and trends of GWR in the five study catchments, illustrated for two classes of groundwater depth (filled bars: depth ≤ 3 m, hollow bars: depth > 3 m). The results are based on the observations at the climate stations in Potsdam, Lindenberg, Angermünde and Marnitz. a) Area-weighted average of GWR per depth class, b) area-weighted trend of GWR per depth class, c) percentage of groundwater depth classes in the catchment area, d) relative contribution of each depth class to the overall trend in GWR.

It was As already pointed out before that in section 1, areas with shallow groundwater tables are generally characterised by high evapotranspiration rates. Therefore, such areas act towards a lower net GWR at the catchment scale (Fig. 7a), and are also expected to respond, due to higher water availability, more strongly to any trend in potential evapotranspiration (see section 4.1). Fig. 7b-c impressively demonstrates this behaviour for all five study catchments. Looking at: the average GWR trend in areas with groundwater depths ≤ 3 m (filled bars), the relative contribution of such areas to the catchment's GWR trend is much higher than in those areas with groundwater depths > 3 m (Fig. 7d) is substantially higher than the actual proportion of these areas in b). Even though areas with groundwater tables < 3 m only account for a smaller fraction of the catchment area (Fig. 7c). The relative contribution of such areas with shallow groundwater tables to the overall GWR trend in the catchment is b), their contribution to the GWR trend of the entire catchment is hence considerably higher (at least 70 % for all catchments:) than the contribution of areas with groundwater tables deeper than 3 m.

5 Limitations and uncertainties

In the previous section, we demonstrated the interplay of some factors that we expect to govern historical trends in simulated GWR: an increase in potential evapotranspiration (driven mainly by rising air temperature and solar irradiation) translates, particularly in areas with a close-shallow groundwater table, to a rise in actual evapotranspiration and hence a net decline in GWR at the catchment scale. An increasing LAI further pushes GWR trends towards negative values by enhancing transpiration and interception losses. Yet, these GWR trends are moderated by incoherent positive and negative precipitation trends that, even though not being statistically significant, can drive GWR trends in the corresponding direction. As a result, a gap appears to remain between the simulated GWR trends and the more negative trends in observed discharge. What could be the causes

455 behind such a gap? Is it merely an issue of statistical significance, with time series of limited length, or are there any processes
not yet sufficiently captured?

Certainly, the chosen approach is affected by various assumptions, simplifications, and uncertainties which might limit the
validity of the resulting GWR trends. In the following, we discuss some of these limitations, and how to maybe address them
in prospective research, in order to allow for a more robust answer to our overarching question of why GWR is decreasing in
460 Brandenburg.

5.1 Length of period for trend analysis

In their study using 28 years of groundwater level data, Lischeid et al. (2021) raised the concern that some of the apparent
trends may have been ~~by~~-caused by frequency-dependent dampening of low-frequency patterns. In our study, a longer time
series of 43 years was used, which should less likely to be concerned by such an effect. Still, discharge and specifically
465 precipitation exhibit a strong inter-annual variability so that even longer time series would be desirable for trend analysis.
While precipitation observations are available long before 1980 at a few gauges (see medium-sized triangles in Fig. 6), this
is not the case for discharge observations for most catchments in Brandenburg. It should also be noted that we required an
exceptionally long spin-up period (from 1951 to 1980) during which the model had to be driven with consistent data in order
to properly initialise the deep unsaturated zone.

470 But even in the presence of longer observational records, it might still be preferable to focus trend analysis on the period
since 1980. This is because an overall regime shift appears to have occurred since then (Reid et al., 2016), which implies
the coincidence of pronounced trends not only in temperature, but, e.g., solar irradiation ("atmospheric brightening" since
the 1980s, after having experienced dimming in the preceding decades), wind speed ("terrestrial stilling"), and LAI (land use
changes and "earth greening"). Hence, there is a trade-off between getting more robust statistics on longer time periods and the
475 aim to capture the accelerated dynamics of climate change (NOAA, 2023) by putting a stronger focus on the recent decades.

5.2 Inhomogeneity of observational series

The observation of all climate variables as well as discharge can be affected by various sources of inhomogeneities, from
changes in the measurement location itself or its surrounding, or changes in the instrumentation (Peterson et al., 1998). In our
study, we did not apply any general homogeneity testing or homogenization techniques. Yet, we attempted, to minimize some
480 specific sources of inhomogeneity, e.g., with regard to solar irradiation and wind speed (see section 3.2. Still, we consider
the uncertainties and the potential for inhomogeneities for these variables as high. For wind, one alternative would be to use
reanalysis data instead of observations. However, initial tests using ERA5-Land-data (Muñoz Sabater et al., 2021) showed that
these fail in reproducing observed average wind speeds and the effect of terrestrial stilling, which are important aspects both
with regard to evapotranspiration and precipitation correction, as demonstrated before.

485 For precipitation, we applied the correction according Kochendorfer et al. (2017) which accounts for temperature and wind
speed, and should hence address inhomogeneities caused by a long-term change of wind-induced undercatch and changing
fractions of solid precipitation. Given the uncertainties introduced by the reconstruction of wind data, as well as changes

in instruments and their immediate vicinity, we assume that the precipitation records might still be subject to substantial inhomogeneity (DWD, personal communication). While it will always be difficult to remove such inhomogeneity, it might be possible to identify specifically spurious gauges by homogeneity tests and by investigating station metadata in more detail.

5.3 The role of land cover and vegetation change

Land cover change is known to have a substantial impact on the water balance (e.g., Zhang et al., 2001), so any transient change in land cover can cause a trend in actual evapotranspiration and hence deep percolation and GWR. Land cover change could imply changes in land cover type (e.g., by conversion from forest to agriculture or reverse) or changes in vegetation properties of an existing land cover type (e.g. by growth or degradation). The transient change of vegetation can act, e.g., through a change in LAI (which affects interception, transpiration, and albedo), a change in water-use efficiency due to higher CO₂-levels, or a change in the effective rooting depth ([Somogyvári et al. \(2024\) have confirmed the importance of vegetation changes, as reflected by a changing NDVI, for the dynamics of a groundwater-fed lake system in Brandenburg](#)). While we have shown that, in fact, Brandenburg experienced a significant increase in LAI over the past 40 years, the reasons for this change are not yet understood. Potential hypotheses are forest regrowth (after widespread clear cuts after World War II), a shift towards maize cropping, a shift towards longer growing seasons due to higher temperatures, or a general greening due to increasing CO₂ concentrations (Zhu et al., 2016). However, vegetation changes are not limited to changes in LAI. Rooting depth is another key variable, which has a profound effect on transpiration and hence the total water deficit in the soil column before the wintery recharge phase. There is evidence that vegetation can quickly adapt to soil water stress with deeper roots (Fan et al., 2017; Li et al., 2024). A climate-change induced increase in soil water depletion could hence be amplified by deeper roots, leading to a positive feedback that increases actual evapotranspiration and hence decreases GWR. However, actual observations or even time series are scarce, so that any potential trends in rooting depth are almost impossible to quantify for the study area.

5.4 Water consumption by irrigation

Irrigated agriculture is not considered in our model setup; yet, an increase in irrigation water withdrawal or an expansion of irrigated areas could, in theory, contribute to a decline in discharge and groundwater levels. However, there is some evidence that this has not been the case in Brandenburg during the considered time period. Simon (2009) comprehensively reported on the temporal development of irrigated areas and irrigated water volumes in eastern Germany before and after the German reunification: In Brandenburg, irrigated areas increased from a value of 1050 km² in 1983 to 1206 km² in 1989, but then collapsed to a value of 200 km² in 1990, followed by more than 30 years in which irrigated areas varied roughly between 200 and 300 km² ([309 km² in 2022, see Amt für Statistik Berlin-Brandenburg, 2024](#)). These numbers do not provide any explanation for decreasing discharges: first, irrigated areas decreased by around 80 % after the 1990. Second, an irrigated area of 200-300 km² corresponds to a water volume of only 20-30 million m³ a⁻¹ (assuming an average annual application of between 70 and 120 mm and its complete evapotranspiration, see Simon, 2009; Amt für Statistik Berlin-Brandenburg, 2012). This volume corresponds to a water depth of around 1 mm a⁻¹ if referred to all of Brandenburg. So even with much higher annual applica-

520 tion rates, irrigation dynamics since 1990 do not have the potential to explain any significant part of the observed water balance changes of the past 40 years.

5.5 Direct anthropogenic interventions in the catchments' water balance

As pointed out in section 2.2, we chose catchments and discharge gauges for which we expect direct anthropogenic interference (e.g., by channelized water transfers) with the catchments water balance to be small. Although we cannot exclude the possibility
525 of such interference, the chances that they will produce more negative discharge trends in all selected catchments are, in our opinion, low. The only catchment for which we actually found a potential effect is the Nuthe catchment: until the 1980s, sewage irrigation fields were operated in the east of the Nuthe catchment near the city of Großbeeren. According to LUA Brandenburg (1997), the corresponding transfer into the Nuthe catchment amounted to around 41 million $\text{m}^3 \text{a}^{-1}$ which amounts to roughly 23 mm a^{-1} at the scale of the receiving Nuthe catchment. While sewage irrigation was discontinued after 1990, it was replaced
530 by a transfer of clear water from the sewage treatment plant Waßmansdorf, directly into a tributary of the Nuthe. According to Möller and Kade (2005), this transfer nominally amounts to 0.4 m^3 under dry and up to 1.3 $\text{m}^3 \text{s}^{-1}$ under rainfall conditions, corresponding to a range of 7–23 mm a^{-1} at the catchment scale. Overall, this could imply a maximum decrease of sewage water transfer into the Nuthe after 1990 of up to 16 mm a^{-1} . Referred to the entire period from 1980 to 2023, this could account for a maximum trend component of around -4 of the observed -13 $\text{mm a}^{-1} \text{dec}^{-1}$.

535 5.6 Uncertainties and changes in groundwater depth

Due to permeable soils and low rainfall, actual evapotranspiration in the study area is largely limited by water availability. However, this does not apply in areas with shallow groundwater tables where plants can transpire at maximum rates. Thus, the groundwater depth fundamentally controls the level at which the positive trend in potential evapotranspiration translates to actual evapotranspiration. Any systematic bias in our groundwater depth data would hence propagate to the trend in actual
540 evapotranspiration (although we are not aware of such a bias).

Correspondingly, any temporal dynamics of groundwater depth in areas with shallow groundwater could affect the water balance (be it on the seasonal or decadal scale) and hence also propagate to the trend in actual evapotranspiration. Yet, groundwater tables in areas of shallow groundwater appeared to be quite stable in the past decades (see section 1) as they are mostly coupled to surface water bodies and stabilised by their hydraulic regulation.

545 Some areas with shallow groundwater may be affected by rising groundwater levels, after drainage practices were progressively being discontinued over the past 30 decades – which would correspond to an increase in actual evapotranspiration. This specifically applies to areas with wetland rehabilitation efforts. For instance, pumping stations have been decommissioned in the Nuthe catchment, leading to re-wetting of areas (LfU Brandenburg, 2025a). At the state level, around 4000 ha of the current total of 6700 ha of wet boglands are based on rehabilitation (LfU Brandenburg, 2025b; MLEUV Brandenburg, 2025). Until
550 2045, 188,000 ha of boglands are planned to be restored (MLEUV Brandenburg, 2025). To assess the implications for the state's water balance, prospective research also needs to account for the possibility that a rise of groundwater in a restoration area could propagate beyond its fringes, and consequently enhance evapotranspiration at larger spatial extents.

5.7 Model uncertainty

The SWAP model features a large number of parameters, many of which are difficult to quantify, and, at the same time, are quite sensitive with regard to the water balance (Wesseling et al., 1998; Baroni and Tarantola, 2014; Stahn et al., 2017). This specifically applies to the soil hydraulic and vegetation parameters (which, e.g., control rooting depth and LAI). As pointed out in section 3.4, we did not carry out a calibration, but set parameter values from literature or independent datasets instead. However, Altdorff et al. (2024) used the very same model implementation and confirmed that it could well reproduce observed local soil water dynamics in the rooting zone across eight monitoring locations in Brandenburg (which cover the main land use and soil types as well as shallow and deep groundwater conditions). While this increases our confidence in the model, our implementation of the hydrotope concept is admittedly simple: by considering only two vegetation types (pine forest and grass-/cropland) and one dominant soil type per catchment, specific effects of soils, crop types or forest traits might not be fully captured by our model setup.

In addition, the uncertainty of soil hydraulic parameters could not only affect the trend of water entering deep percolation, but also the transit times of this water towards the groundwater table (particularly for deep unsaturated zones of several decameters), and hence the temporal distribution of simulated GWR. However, preliminary tests suggested that these delays only have limited effects on the computed trends on the catchment scale. Finally, our model setup does not account for the water flow within the aquifer, which involves an additional dampening of the signal and a further increase of travel time until the water emerges in surface water bodies.

So while the model itself as well as its setup and parameterisation in the present study context implies a range of uncertainties, it remains unclear whether and in which direction these uncertainties would affect the simulated trends in GWR. For this purpose, a comprehensive uncertainty and sensitivity assessment with specific attention to GWR trends would be desirable, but is beyond the scope of the present study.

6 Conclusions

Time series of river discharge and ~~ground-water~~groundwater levels provide strong evidence that GWR is decreasing since 1980 in large parts of the federal state of Brandenburg, Germany. So far, however, no simulation study did confirm any such negative GWR trend.

In our study, we used a combination of model and data specifically tailored to the situation in Brandenburg with its highly permeable soils, low relief, and a mix of very shallow and deep aquifers. Furthermore, we paid special attention to use homogeneous climate forcing data, to transparently account for the uncertainty of precipitation trends, and, based on a recently published dataset, to consider the effect of a long-term LAI increase on the water balance.

For five catchments across Brandenburg, we found that significant increases of air temperature, solar irradiation and LAI since 1980 acted towards a decrease in GWR in the order of -21 to -4 mm a^{-1} per decade. The contribution of the LAI trend ($+0.1$ $\text{m}^2 \text{m}^{-2}$ per decade) amounted to 3 – 5 mm a^{-1} per decade. Based on these results, we consider it as very likely that the

585 decrease in discharge since 1980 can be explained by a decrease in GWR which, in turn, was caused by climate change in combination with an increasing LAI.

However, we also found that trends from alternative precipitation times series can be highly incoherent at the catchment scale (partly ranging over more than 20 mm a^{-1} per decade). Even though none of these precipitation trends are significant, they can have a fundamental impact on the significance, the magnitude and even on the sign of simulated GWR trends.

590 Given the uncertainty of the precipitation trends, four out of five catchments still appear to exhibit a gap between the negative simulated GWR trends and the more negative observed discharge trends. While we could not explain this gap with certainty, we comprehensively discussed possible reasons, including the effects of the limited length and the inhomogeneity of climate and discharge records, the role of land cover and vegetation change, irrigation water consumption, more latent anthropogenic interventions in the catchments' water balance, uncertainties in ~~ground-water~~ groundwater table depth, as well as model-related
595 uncertainties. Addressing these uncertainties should be a prime subject for prospective research.

Given that the trend in simulated GWR is highly sensitive to any trend in precipitation, and that, at the same time, any precipitation trend in future climate projections is known to be highly uncertain and often not significant, we conclude that future projections on GWR trends for Brandenburg need to be interpreted with greatest caution. Marx et al. (2024) suggested that GWR in Brandenburg will increase in the future; however, the aforementioned discrepancies between models and observations
600 for the past decades do not lend much credibility to such an optimistic outlook.

But what does it mean for water resources management and planning in Brandenburg if we neither can trust in a stable or even increasing GWR, nor safely expect a future decrease? Of course, this kind of uncertainty is putting any decision-maker in an inconvenient position. In the light of this uncertainty, our recommendation is to put a stronger focus on monitoring: understanding historical and contemporary dynamics of water availability, based on a combination of models and observations,
605 is our best shot at anticipating critical situations with the required level of certainty. For the current situation, this means: there is very strong evidence that we are in a phase of a climate-induced decrease of GWR, so we should act accordingly.

Data availability. All data sets used for model setup and forcing are openly available. The sources of the corresponding datasets are outlined in detail in section 2.

Author contributions. Both authors contributed equally in developing the study concept, carrying out the data processing and analysis,
610 producing the figures and writing the manuscript.

Competing interests. The corresponding author declares that none of the authors has competing interests.

Acknowledgements. This research was funded by the Ministerium für Landwirtschaft, Umwelt und Klimaschutz des Landes Brandenburg (MLUK, Ministry of Agriculture, Environment, and Climate Protection of the federal state of Brandenburg) as well as by the Deutsche Forschungsgemeinschaft (DFG, German Research Foundation) – research unit FOR 2694 "Cosmic Sense", project number 357874777. We
615 thank Rebekka Eichstädt (LfU Brandenburg) for helpful discussions on trends of climatic variables and groundwater recharge.

References

- Altdorff, D., Heistermann, M., Francke, T., Schrön, M., Attinger, S., Bauriegel, A., Beyrich, F., Biró, P., Dietrich, P., Eichstädt, R., Grosse, P. M., Markert, A., Terschläsen, J., Walz, A., Zacharias, S., and Oswald, S. E.: Brief Communication: A new drought monitoring network in the state of Brandenburg (Germany) using cosmic-ray neutron sensing, *EGUsphere*, <https://doi.org/10.5194/egusphere-2024-3848>, publisher: Copernicus GmbH, 2024.
- 620 Amt für Statistik Berlin-Brandenburg: Flächenerhebung nach Art der tatsächlichen Nutzung in Berlin und Brandenburg, <https://www.statistik-berlin-brandenburg.de/a-v-3-j>, last accessed: 6 January 2025, 2023.
- Amt für Statistik Berlin-Brandenburg: Statistischer Bericht, C IV 11 – u / 09, Bewässerung in landwirtschaftlichen Betrieben im Land Brandenburg 2009, https://opus4.kobv.de/opus4-slbp/files/3102/SB_C04_11_00_2009u00_BB.pdf, last accessed: 9 May 2025, 2012.
- 625 Amt für Statistik Berlin-Brandenburg: Pressemitteilung Nr. 71, <https://www.statistik-berlin-brandenburg.de/071-2024>, last accessed: 9 May 2025, 2024.
- Anderson, K., Hansen, C., Holmgren, W., Jensen, A., Mikofski, M., and Driesse, A.: pvlib python: 2023 project update, *Journal of Open Source Software*, 8, 5994, <https://doi.org/10.21105/joss.05994>, 2024.
- Baroni, G. and Tarantola, S.: A General Probabilistic Framework for uncertainty and global sensitivity analysis of deterministic models: A hydrological case study, *Environmental Modelling Software*, 51, 26–34, <https://doi.org/10.1016/j.envsoft.2013.09.022>, 2014.
- 630 Cao, S., Li, M., Zhu, Z., Wang, Z., Zha, J., Zhao, W., Duanmu, Z., Chen, J., Zheng, Y., Chen, Y., Myneni, R. B., and Piao, S.: Spatiotemporally consistent global dataset of the GIMMS leaf area index (GIMMS LAI4g) from 1982 to 2020, *Earth System Science Data*, 15, 4877–4899, <https://doi.org/10.5194/essd-15-4877-2023>, 2023.
- DWD: Daily station observations (temperature, pressure, precipitation, sunshine duration, etc.) for Germany, version 24.3, https://opendata.dwd.de/climate_environment/CDC/observations_germany/climate/daily/kl/, last accessed: 6 January 2025, 2024a.
- 635 DWD: Daily precipitation observations for Germany, version 24.3, https://opendata.dwd.de/climate_environment/CDC/observations_germany/climate/daily/more_precip/, last accessed: 6 January 2025, 2024b.
- DWD: Raster data set precipitation sums in mm for Germany - HYRAS-DE-PR, version 6.0, https://opendata.dwd.de/climate_environment/CDC/grids_germany/daily/hyras_de/precipitation/, last accessed: 6 January 2025, 2024c.
- 640 Fan, Y., Miguez-Macho, G., Jobbágy, E. G., Jackson, R. B., and Otero-Casal, C.: Hydrologic regulation of plant rooting depth, *Proceedings of the National Academy of Sciences*, 114, 10 572–10 577, <https://doi.org/10.1073/pnas.1712381114>, 2017.
- Gash, J. H. C., Lloyd, C. R., and Lachaud, G.: Estimating sparse forest rainfall interception with an analytical model, *Journal of Hydrology*, 170, 79–86, [https://doi.org/10.1016/0022-1694\(95\)02697-N](https://doi.org/10.1016/0022-1694(95)02697-N), 1995.
- Guan, H. and Wilson, J. L.: A hybrid dual-source model for potential evaporation and transpiration partitioning, *Journal of Hydrology*, 377, 405–416, <https://doi.org/10.1016/j.jhydrol.2009.08.037>, 2009.
- 645 Guerrero-Ramírez, N. R., Mommer, L., Freschet, G. T., Iversen, C. M., McCormack, M. L., Kattge, J., Poorter, H., van der Plas, F., Bergmann, J., Kuyper, T. W., York, L. M., Bruelheide, H., Laughlin, D. C., Meier, I. C., Roumet, C., Semchenko, M., Sweeney, C. J., van Ruijven, J., Valverde-Barrantes, O. J., Aubin, I., Catford, J. A., Manning, P., Martin, A., Milla, R., Minden, V., Pausas, J. G., Smith, S. W., Soudzilovskaia, N. A., Ammer, C., Butterfield, B., Craine, J., Cornelissen, J. H. C., de Vries, F. T., Isaac, M. E., Kramer, K., König, C., Lamb, E. G., Onipchenko, V. G., Peñuelas, J., Reich, P. B., Rillig, M. C., Sack, L., Shipley, B., Tedersoo, L., Valladares, F., van Bodegom, P., Weigelt, P., Wright, J. P., and Weigelt, A.: Global root traits (GRoOT) database, *Global Ecology and Biogeography*, 30, 25–37, <https://doi.org/10.1111/geb.13179>, 2021.

- Hofstra, N., New, M., and McSweeney, C.: The influence of interpolation and station network density on the distributions and trends of climate variables in gridded daily data, *CLIMATE DYNAMICS*, 35, 841–858, <https://doi.org/10.1007/s00382-009-0698-1>, 2010.
- 655 Holmgren, W., Hansen, C., and Mikofski, M.: pvlb python: a python package for modeling solar energy systems, *Journal of Open Source Software*, 3, 884, <https://doi.org/10.21105/joss.00884>, 2018.
- Kochendorfer, J., Nitu, R., Wolff, M., Mekis, E., Rasmussen, R., Baker, B., Earle, M. E., Reverdin, A., Wong, K., Smith, C. D., Yang, D., Roulet, Y.-A., Buisan, S., Laine, T., Lee, G., Aceituno, J. L. C., Alastrué, J., Isaksen, K., Meyers, T., Brækkan, R., Landolt, S., Jachcik, A., and Poikonen, A.: Analysis of single-Alter-shielded and unshielded measurements of mixed and solid precipitation from WMO-SPICE, *Hydrology and Earth System Sciences*, 21, 3525–3542, <https://doi.org/10.5194/hess-21-3525-2017>, publisher: Copernicus GmbH, 2017.
- 660 Kröcher, J., Ghazaryan, G., and Lischeid, G.: Unravelling Regional Water Balance Dynamics in Anthropogenically Shaped Lowlands: A Data-Driven Approach, *Hydrological Processes*, 39, e70 053, <https://doi.org/https://doi.org/10.1002/hyp.70053>, e70053 HYP-24-0611.R2, 2025.
- Kroes, J., van Dam, J., Bartholomeus, R., Groenendijk, P., Heinen, M., Hendriks, R., Mulder, H., Supit, I., and van Walsum, P.: SWAP version 4 - Theory description and user manual, Wageningen Environmental Research Report 2780, https://swap.wur.nl/Documents/Kroes_et_al_2017_SWAP_version_4_ESG_Report_2780.pdf, last accessed: 6 January 2025, 2017.
- 665 Landesamt für Umwelt Brandenburg: Wasserversorgungsplanung Brandenburg - Sachlicher Teilabschnitt mengenmäßige Grundwasserbewirtschaftung, https://lfu.brandenburg.de/sixcms/media.php/9/Wasserversorgungsplan_barrierefrei.pdf, 2022.
- LBGR: Landesamt für Bergbau, Geologie und Rohstoffe Brandenburg, Bodenübersichtskarte des Landes Brandenburg im Maßstab 1:300,000, <https://geo.brandenburg.de/?page=LBGR-Webservices>, last accessed: 18 September 2024, 2024.
- 670 LFU: Landesamt für Umwelt Brandenburg, Mächtigkeit der ungesättigten Bodenzone, <https://metaver.de/trefferanzeige?docuuiid=06BE213C-BE2F-4009-8208-C58771700A33>, last accessed: 18 September 2024, 2013.
- LfU Brandenburg: FFH-Gebiet und SPA Nuthe-Nieplitz-Niederung - Naturpark Nuthe-Nieplitz, <https://www.nuthe-nieplitz-naturpark.de/themen/natura-2000/ffh-gebiet-und-spa-nuthe-nieplitz-niederung/>, 2025a.
- 675 LfU Brandenburg: Moorschutz in Brandenburg im Vergleich mit anderen Bundesländern | Startseite | LfU, <https://lfu.brandenburg.de/lfu/de/aufgaben/boden/moorschutz/grundlagen-moorschutz/moorschutz-in-brandenburg-im-vergleich-mit-anderen-bundeslaendern/>, 2025b.
- Li, B., Wang, X., and Li, Z.: Plants extend root deeper rather than increase root biomass triggered by critical age and soil water depletion, *Science of The Total Environment*, 914, 169 689, <https://doi.org/10.1016/j.scitotenv.2023.169689>, 2024.
- Lischeid, G., Dannowski, R., Kaiser, K., Nützmann, G., Steidl, J., and Stüve, P.: Inconsistent hydrological trends do not necessarily imply spatially heterogeneous drivers, *Journal of Hydrology*, 596, 126 096, <https://doi.org/https://doi.org/10.1016/j.jhydrol.2021.126096>, 2021.
- 680 LUA Brandenburg: Rieselfelder südlich Berlins, Studien- und Tagungsbericht Band 13/14, <https://lfu.brandenburg.de/sixcms/media.php/9/STUDIEN%20Band%2013-14%3D1.pdf>, last accessed: 6 January 2025, 1997.
- LUA Brandenburg: Flächendeckende Modellierung von Wasserhaushaltsgrößen für das Land Brandenburg - Studien und Tagungsberichte, Band 27 | Startseite | LfU, Tech. Rep. Band 27, Landesumweltamt Brandenburg, <https://lfu.brandenburg.de/lfu/de/ueber-uns/veroeffentlichungen/detail/~15-10-2001-flaechendeckende-modellierung-von-wasserhaushaltsgroessen-fuer-das-land-brandenburg-stu#>, 2001.
- 685 Marx, A., Boeing, F., Rakovec, O., Müller, S., Can, O., Malla, C., Peichl, M., and Samaniego, L.: Auswirkungen des Klimawandels auf Wasserbedarf und -dargebot, *WasserWirtschaft*, 111, 14 – 19, <https://doi.org/10.1007/s35147-021-0905-5>, 2024.
- MLEUV Brandenburg: Moorschutz | MLUK, <https://mluk.brandenburg.de/mluk/de/umwelt/wasser/moorschutz/>, 2025.

- 690 Möller, K. and Kade, N.: Behandeltes Abwasser als Ressource Die Südaleitung als Beitrag zur Stützung des Landschaftswasserhaushaltes in der Nuthe-Notte-Niederung: Erfahrungen mit der Ableitung weitergehend gereinigten Abwassers aus dem Klärwerk Waßmannsdorf, Schriftenreihe Kompetenzzentrum Wasser Berlin Band 3, <https://digital.zlb.de/viewer/api/v1/records/33661377/files/images/abwasser.pdf/full.pdf>, last accessed: 6 January 2025, 2005.
- Muñoz Sabater, J., Dutra, E., Agustí-Panareda, A., Albergel, C., Arduini, G., Balsamo, G., Boussetta, S., Choulga, M., Harrigan, S., Hersbach, H., Martens, B., Miralles, D. G., Piles, M., Rodríguez-Fernández, N. J., Zsoter, E., Buontempo, C., and Thépaut, J.-N.: ERA5-Land: a state-of-the-art global reanalysis dataset for land applications, *Earth System Science Data*, 13, 4349–4383, <https://doi.org/10.5194/essd-13-4349-2021>, 2021.
- 695 NOAA: Global Annual Climate Report 2023, <https://www.ncei.noaa.gov/access/monitoring/monthly-report/global/202313>, last accessed: 6 January 2025, 2023.
- 700 OpenStreetMap contributors: Planet dump retrieved from <https://planet.osm.org>, <https://www.openstreetmap.org>, last access: October 2024., 2024.
- Peterson, T., Easterling, D., Karl, T., Groisman, P., Nicholls, N., Plummer, N., Torok, S., Auer, I., Boehm, R., Gullett, D., Vincent, L., Heino, R., Tuomenvirta, H., Mestre, O., Szentimrey, T., Salinger, J., Forland, E., Hanssen-Bauer, I., Alexandersson, H., Jones, P., and Parker, D.: Homogeneity adjustments of in situ atmospheric climate data: A review, *INTERNATIONAL JOURNAL OF CLIMATOLOGY*, 18, 1493–1517, [https://doi.org/10.1002/\(SICI\)1097-0088\(19981115\)18:13<1493::AID-JOC329>3.0.CO;2-T](https://doi.org/10.1002/(SICI)1097-0088(19981115)18:13<1493::AID-JOC329>3.0.CO;2-T), 1998.
- 705 Pohle, I., Zeilfelder, S., Birner, J., and Creutzfeldt, B.: The 2018–2023 drought in Berlin: impacts and analysis of the perspective of water resources management, *Natural Hazards and Earth System Sciences*, 25, 1293–1313, <https://doi.org/10.5194/nhess-25-1293-2025>, 2025.
- Razafimaharo, C., Krähenmann, S., Höpp, S., Rauthe, M., and Deutschländer, T.: New high-resolution gridded dataset of daily mean, minimum, and maximum temperature and relative humidity for Central Europe (HYRAS), *Theoretical and Applied Climatology*, 142, 1531–1553, <https://doi.org/10.1007/s00704-020-03388-w>, 2020.
- 710 Reid, P. C., Hari, R. E., Beaugrand, G., Livingstone, D. M., Marty, C., Straile, D., Barichivich, J., Goberville, E., Adrian, R., Aono, Y., Brown, R., Foster, J., Groisman, P., Hélaouët, P., Hsu, H.-H., Kirby, R., Knight, J., Kraberg, A., Li, J., Lo, T.-T., Myneni, R. B., North, R. P., Pounds, J. A., Sparks, T., Stübi, R., Tian, Y., Wiltshire, K. H., Xiao, D., and Zhu, Z.: Global impacts of the 1980s regime shift, *Global Change Biology*, 22, 682–703, <https://doi.org/10.1111/gcb.13106>, 2016.
- 715 Richter, D.: Ergebnisse methodischer Untersuchungen zur Korrektur des systematischen Meßfehlers des Hellmann-Niederschlagsmessers, no. 194 in *Berichte des Deutschen Wetterdienstes, Selbstverl. des Dt. Wetterdienstes, Offenbach am Main*, ISBN 3-88148-309-8, <https://dwdbib.dwd.de/38928>, 1995.
- Russ, A., Riek, W., Kallweit, R., Einert, P., Jochheim, H., Lüttschwager, D., Hannemann, J., and Becker, F.: "Wasserhaushalt von Standorten des Level II-Programms in Brandenburg", in: "30 Jahre forstliches Umweltmonitoring in Brandenburg, Eberswalder Forstliche Schriftenreihe Band 63", edited by Kallweit, R. and Engel, J., pp. 135–152, "Ministerium für Ländliche Entwicklung, Umwelt und Landwirtschaft des Landes Brandenburg", 2016.
- 720 Schaap, M. G., Leij, F. J., and van Genuchten, M. T.: ROSETTA: a computer program for estimating soil hydraulic parameters with hierarchical pedotransfer functions, *Journal of Hydrology*, 251, 163–176, [https://doi.org/10.1016/S0022-1694\(01\)00466-8](https://doi.org/10.1016/S0022-1694(01)00466-8), 2001.
- Sen, P. K.: Estimates of the Regression Coefficient Based on Kendall's Tau, *Journal of the American Statistical Association*, 63, 1379–1389, <https://doi.org/10.1080/01621459.1968.10480934>, publisher: ASA Website _eprint: <https://www.tandfonline.com/doi/pdf/10.1080/01621459.1968.10480934>, 1968.
- 725

- Simon, M.: Die landwirtschaftliche Bewässerung in Ostdeutschland seit 1949 - Eine historische Analyse vor dem Hintergrund des Klimawandels, PIK report 114, <https://www.pik-potsdam.de/en/output/publications/pikreports/files/pr114.pdf>, 2009.
- 730 Somogyvári, M., Scherer, D., Bart, F., Fehrenbach, U., Okujeni, A., and Krueger, T.: A hybrid data-driven approach to analyze the drivers of lake level dynamics, *Hydrology and Earth System Sciences*, 28, 4331–4348, <https://doi.org/10.5194/hess-28-4331-2024>, 2024.
- Somogyvári, M., Brill, F., Tsypin, M., Rihm, L., and Krueger, T.: Regional-scale groundwater analysis with dimensionality reduction, *EGU-sphere*, 2025, 1–25, <https://doi.org/10.5194/egusphere-2024-4031>, 2025.
- Stahn, P., Busch, S., Salzmann, T., Eichler-Loebermann, B., and Miegel, K.: Combining global sensitivity analysis and multiobjective optimisation to estimate soil hydraulic properties and representations of various sole and mixed crops for the agro-hydrological SWAP model, *ENVIRONMENTAL EARTH SCIENCES*, 76, <https://doi.org/10.1007/s12665-017-6701-y>, 2017.
- 735 Theil, H.: A rank-invariant method of linear and polynomial regression analysis. I, *Proceedings. Akademie van Wetenschappen Amsterdam. North-Holland, Amsterdam*, 53, 386–392 = *Indagationes Math.* 12, 85–91, 1950.
- Umweltbundesamt: Auswirkung des Klimawandels auf die Wasserverfügbarkeit - Anpassung an Trockenheit und Dürre in Deutschland (WADKlim), https://www.umweltbundesamt.de/sites/default/files/medien/2875/dokumente/143_2024_texte_wadklim.pdf, 2024.
- 740 van Dam, J. C., Groenendijk, P., Hendriks, R. F., and Kroes, J. G.: Advances of Modeling Water Flow in Variably Saturated Soils with SWAP, *Vadose Zone Journal*, 7, 640–653, <https://doi.org/10.2136/vzj2007.0060>, 2008.
- van Genuchten, M. T.: A Closed-form Equation for Predicting the Hydraulic Conductivity of Unsaturated Soils, *Soil Science Society of America Journal*, 44, 892–898, <https://doi.org/10.2136/sssaj1980.03615995004400050002x>, <https://onlinelibrary.wiley.com/doi/pdf/10.2136/sssaj1980.03615995004400050002x>, 1980.
- 745 Vautard, R., Cattiaux, J., Yiou, P., Thépaut, J.-N., and Ciais, P.: Northern Hemisphere atmospheric stilling partly attributed to an increase in surface roughness, *Nature Geoscience*, 3, 756–761, <https://doi.org/10.1038/ngeo979>, publisher: Nature Publishing Group, 2010.
- Von Hoyningen-Huene, J.: Die Interzeption des Niederschlages in landwirtschaftlichen Pflanzenbeständen, *Die Interzeption des Niederschlages in landwirtschaftlichen Pflanzenbeständen*, pp. 1–53, 1983.
- Wesseling, J., Kroes, J., and Metselaar, K.: Global sensitivity analysis of the Soil-Water-Atmosphere-Plant (SWAP) model, Wageningen (The Netherlands), DLO Winand Staring Centre. Report 16, <https://edepot.wur.nl/363800>, last accessed: 6 January 2025, 1998.
- 750 Wild, M.: Global dimming and brightening: A review, *Journal of Geophysical Research: Atmospheres*, 114, <https://doi.org/10.1029/2008JD011470>, <https://onlinelibrary.wiley.com/doi/pdf/10.1029/2008JD011470>, 2009.
- Yang, Y., Roderick, M. L., Guo, H., Miralles, D. G., Zhang, L., Fatichi, S., Luo, X., Zhang, Y., McVicar, T. R., Tu, Z., Keenan, T. F., Fisher, J. B., Gan, R., Zhang, X., Piao, S., Zhang, B., and Yang, D.: Evapotranspiration on a greening Earth, *Nature Reviews Earth and Environment*, 4, 626 – 641, <https://doi.org/10.1038/s43017-023-00464-3>, cited by: 132, 2023.
- 755 Yue, S., Pilon, P., and Cavadias, G.: Power of the Mann–Kendall and Spearman’s rho tests for detecting monotonic trends in hydrological series, *Journal of Hydrology*, 259, 254–271, [https://doi.org/10.1016/S0022-1694\(01\)00594-7](https://doi.org/10.1016/S0022-1694(01)00594-7), 2002.
- Zhang, L., Dawes, W., and Walker, G.: Response of mean annual evapotranspiration to vegetation changes at catchment scale, *Water Resources Research*, 37, 701–708, <https://doi.org/10.1029/2000WR900325>, 2001.
- 760 Zhu, Z., Piao, S., Myneni, R. B., Huang, M., Zeng, Z., Canadell, J. G., Ciais, P., Sitch, S., Friedlingstein, P., Arneeth, A., Cao, C., Cheng, L., Kato, E., Koven, C., Li, Y., Lian, X., Liu, Y., Liu, R., Mao, J., Pan, Y., Peng, S., Penuelas, J., Poulter, B., Pugh, T. A. M., Stocker, B. D., Viovy, N., Wang, X., Wang, Y., Xiao, Z., Yang, H., Zaehle, S., and Zeng, N.: Greening of the Earth and its drivers, *Nature Climate Change*, 6, 791+, <https://doi.org/10.1038/NCLIMATE3004>, 2016.